Structure of mixed-layer corrensite-chlorite revealed by high-resolution transmission electron microcopy (HRTEM)

Toshihiro KOGURE[1], Victor A. DRITS[2] and Sayako INOUE[1]

[1]Department of Earth and Planetary Science, Graduate School of Science, The University of Tokyo, 7-3-1 Hongo, Bunkyo-ku, Tokyo, 113-0033, Japan
[2]Geological Institute of the Russian Academy of Sciences, Pyzhevsky per 7, Moscow, Russia

---

Running title proposed: Structure of corrensite-chlorite revealed by HRTEM

Corresponding author:
Toshihiro Kogure
Department of Earth and Planetary Science, Graduate School of Science,
The University of Tokyo
7-3-1 Hongo, Bunkyo-ku, Tokyo 113-0033, Japan
E-mail: kogure@eps.s.u-tokyo.ac.jp

Revision 2

Submitted
January 2013

ABSTRACT

Mixed-layer corrensite-chlorite in a glauconitic sandy-clayey rock has been investigated and the three-dimensional stacking structure of corrensite was determined for the first time using high-resolution transmission electron microscopy (HRTEM), as well as suggesting the corrensite-chlorite transition mechanism. The crystals consist of corrensite and chlorite packets excluding successive smectite layers, consistent with the result of XRD analysis previously reported for the same specimen. One-dimensional HRTEM imaging of corrensite with dark contrast corresponding to the cation sheets indicated two types of the smectite-like interlayers in corrensite, probably containing one atomic plane and without any distinct material, which results in the corrensite basal heights of ca. 26.5 Å and 24.4 Å, respectively, in TEM. Two-dimensional HRTEM imaging revealed that the polytypic stacking sequence in the chlorite-like layer (the two 2:1 layers and the brucite-like sheet (B-sheet) between them) in the corrensite unit is always II*bb* type. The intralayer displacements of the two 2:1 layers in the unit are well-ordered to show a "two-layer" character, which can be regarded as combination of two different one-layer chlorite polytypes belonging to II*bb*. These regulated features of corrensite structure support the proposals in previous works that corrensite has a thermodynamic stability field and precipitated directly from solution probably in an environment with a high water/rock ratio, without inheriting smectite structures, during the smectite-to-chlorite transition. The number of the successive B-sheets in the corrensite-chlorite interstratification is always odd. Along with frequent observation of the transition from the smectite-like interlayer to the B-sheet and similarity of polytypic stacking sequence between corrensite and chlorite, this result strongly supports the transformation from corrensite to chlorite, by replacing the smectite-like interlayer with the B-sheet.

Key Words: corrensite, chlorite, mixed-layer minerals, polytypic stacking sequence, transformation, HRTEM

INTRODUCTION

Corrensite is a trioctahedral 2:1 phyllosilicate with 1:1 ordered interstratifications of chlorite and smectite (or vermiculite) layers. The mineral name "corrensite" is usable for specimens with a high "rationality" for 00*l* reflections in their X-ray diffraction (XRD) patterns beside the low-angle 001 reflection with $d \sim 28$ Å, otherwise they are usually called mixed-layered or interstratified chlorite-smectite/vermiculite (Bailey, 1982; Reynolds, 1988). Geological occurrences of corrensite reported to date are diverse but often related to prograde or retrograde transition between smectite (saponite) and chlorite (Reynolds, 1988; Beaufort et al., 1997; Drits et al., 2011). Among them, prograde transitions from smectite to chlorite in burial diagenesis, hydrothermal alteration, contact- or regional metamorphism, etc. in rocks with mafic compositions were given the most attention, as the counterpart of dioctahedral smectite to illite transitions.

Two modes were suggested or reported for such prograde smectite-to-chlorite transition. In one of them the transition proceeds through mixed-layer smectite-chlorite (S-C), in which the content of chlorite layers continuously increases from 0 to 100% following the similar layer stacking sequences observed in illite-smectite subjected to burial diagenesis (Reynolds, 1980; Bettison and Schiffman, 1988; Chang et al., 1986). The second is stepwise evolution of the transition with gaps restricting possible concentration of the interstratified layer types in S-C structures (Drits and Sakharov, 1976; Kossovskaya and Drits, 1985; Inoue et al., 1984; Inoue, 1987; Drits and Kossovskaya, 1990; Inoue and Utada, 1991). This stepwise evolution has been well explained by the formation of corrensite with a particular thermodynamical stability field and defined phase relations with smectite, vermiculite and chlorite (Velde, 1977; Reynolds, 1988; Shau et al., 1990; Beaufort et al., 1997; Shau and Peacor, 1992; Murakami et al., 1999). In this case, the clays with < 50% or > 50% chlorite layers should be interstratifications of either smectite-corrensite (S-Co) or corrensite-chlorite (Co-C), and a random S-C interstratification does not exist. It was suggested that the selection between the two different modes is related to water/rock ratios in the microenvironments where the transition proceeds (Shau and Peacor, 1992; Bettison-Varga and Mackinnon, 1997). However, it seems that important details of the transition, and its structural pathways and mechanisms are still not understood completely.

XRD, high-resolution transmission electron microscopy (HRTEM) and especially their combination are the most powerful tools to investigate mixed-layer phyllosilicate minerals including the mixed-layer S-C, as evidenced by the many previous works cited above. However, it seems that more accurate and/or detailed analyses are necessary to characterize these minerals. For example, interpretation of the experimental XRD patterns has been based on their simulation using the NEWMOD program (Reynolds, 1985), decomposition of broad and asymmetrical basal reflections, or both (e.g., Beaufort et al., 1997; Leoni et al., 2010). In these investigations, the structural models were restricted by mixed-layer S-C and Co-C having either random (R = 0) or ordered (R = 1) interstratification of the layer types. Moreover, identification of corrensite as the periodic structure is usually based on the value of the coefficient of variation (CV) describing the deviation from the rationality for 00*l* reflections. According to Bailey (1982) criterion the sample with CV ≤ 0.7% can be considered as a periodic corrensite. It turned out that these approaches failed to provide unambiguous interpretation of the experimental XRD data (e.g. Beaufort et al., 1997).

With respect to HRTEM, many previous works (e.g., Shau and Peacor, 1992; Beaufort et al., 1997; Bettison-Varga and Mackinnon, 1997) recorded only one-dimensional lattice images to show the distribution of different layer types in crystals. Although these images are still valuable to observe "directly" the structure of mixed-layer minerals, they cannot display three-dimensional stacking structures or polytypic aspects of phyllosilicates. It was demonstrated that detailed analyses of the polytypic stacking sequences in mixed-layer phyllosilicates using two-dimensional HRTEM images could reach reliable transition models for serpentine-chlorite (Banfield and Bailey, 1996), chlorite-vermiculite (Banfield and Murakami, 1998) and biotite-chlorite (Kogure and Banfield, 2000). However, with respect to mixed-layer S-C or Co-C, similar HRTEM analyses have been never. Even the three-dimensional "crystal" structure of corrensite has not been reported, probably because of its fine particle size and highly-defective structure.

In this situation, Drits et al. (2011) investigated extensively mixed-layer corrensite-chlorite formed in the cement of glauconitic sandstone-clayey rocks, mainly using XRD and X-ray chemical analyses. In particular, their detailed XRD analyses have shown that one of the studied specimen in ethylene-glycolated state with CV = 0.17% as corrensite actually contains 40% chlorite and 60% corrensite units. Moreover, in contrast to the previous works, their modeling has reproduced perfectly the positions, intensities and profiles of basal reflections in the experimental XRD patterns, using the model in which Co and C components are interstratified at R = 1 with a significant tendency to segregation with P_{chch} = 0.75, where P_{chch} is the conditional probability for the continuity of the chlorite layers (Drits et al., 2011). This result suggests that Bailey' criterion must be used with high caution.

In the present study, we further analyzed the same sample using TEM, to verify the mixed-layer structure model derived by the XRD analysis. Furthermore, beyond this purpose, we determined the three-dimensional stacking structure of corrensite, which has not been reported yet, using distinct two-dimensional HRTEM images along the two principal zone axes (Kogure and Nespolo, 1999a, 1999b, Kogure et al., 2008). Finally, from the stacking structures of corrensite and intercalated chlorite, we discuss the corrensite-chlorite transition model.

SAMPLES AND METHODS

The specimen investigated was mixed-layer corrensite-chlorite that forms brownish grains of 0.1-0.4 mm (sample 500L) in a glauconitic sandy-clayey rock, taken from the basal portion of the lower subformation of the Yusmastakh Formation (Riphean, Anabar Uplift, North Siberia) (Drits et al., 2011).

The specimens for TEM examination with the electron beam parallel to the layers were prepared using the method described in Kogure (2002). The powdered specimen was embedded with epoxy resin between two glass slides. After hardening, the glass slides were cut using a diamond wheel to laths of ~ 1 mm thick. The laths were thinned to ~ 70 μm by mechanical grinding and then argon ion milled. HRTEM examination was performed at 200 kV using a JEOL JEM-2010 UHR with a nominal point resolution of ca. 2 Å. Images were recorded on films or Gatan MSC 794 bottom-mounted CCD camera. HRTEM images were taken at sufficiently thin regions of the specimen. The defocus value was adjusted to record the contrast that corresponds to the projected potential of the crystal structure (Kogure 2002). The corrensite parts were beam sensitive and amorphization proceeded during HRTEM recording. Noisy contrast from amorphous materials in HRTEM images was removed using a Wiener-filter (Marks 1996; Kilaas 1998) developed by K. Ishizuka (HREM Research Inc.) and implemented with Gatan DigitalMicrograph version 3.1 0.0 (Kogure et al., 2008).

RESULTS AND DISCUSSION

Identification of corrensite with two types of smectite-like interlayers and interstratified chlorite

Generally the corrensite-chlorite layers are often curved in their cross-sectional views. Lenticular microcleavages are common in the crystals, which were presumably formed by the collapse of hydrated smectite-like interlayers in the vacuum environment during ion-milling or TEM examination. Energy dispersive X-ray analyses in TEM for many grains indicated that they are categorized as Mg or Mg-Fe compositional variety described in Drits et al. (2011). HRTEM with proper defocus and orientation reveals one-dimensional lattice images by using only 00*l* reflections, or two-dimensional ones if the incident beam is along one of $\pm X_i$ or $\pm Y_i$ directions (Bailey, 1988a), in which the brucite-like hydroxide sheets (hereafter called "B-sheet") in corrensite and chlorite are unambiguously identified as the boldest dark lines, as indicated by the arrows with "B" in Figure 1 (e.g., Bons and Schryvers, 1989; Banfield and Bailey, 1996; Kogure and Murakami, 1998). The chlorite packets are commonly identified with successive interlayers with B-sheets and ca.14 Å periodicity, which supports well our previous XRD analysis (Drits et al., 2011) that although the corrensite basal 00*l* reflections are highly rational with the coefficient of variation (CV) of 0.3 % (air-dried state) or 0.17% (ethyleneglycolated state), the specimen is not pure corrensite but contains 40% chlorite units. On the other hand, alternating B-sheets at the interlayers indicate corrensite packets. B-sheets separated by more than one smectite-like interlayer were never observed, confirming that the specimen is definitely the interstratifications of corrensite and chlorite (Co-C), not smectite and chlorite (S-C). Corrensite units or chlorite layers with different orientations sharing (001) planes are often interstratified in a crystal (Fig. 1). The boundaries of such different layer orientation are always at the smectite-like interlayers in corrensite, as indicated with the arrows "1" and "2" in Figure 1.

Careful examination of the images revealed the existence of two types of smectite-like interlayers in the specimen (Fig. 1b). In the figure, six or seven dark thin lines are observed between the adjacent B-sheets. Among them, six lines must correspond to tetrahedral and octahedral sheets in the two 2:1 layers. Hence, one extra line among the seven thin lines should correspond to one atomic plane at the interlayer. Hereafter this interlayer is denoted as I_w (smectite-like **I**nterlayer with a **W**ider space) and that without the dark line as I_n (with a **N**arrower space). The basal height of one corrensite unit with I_w is 26.5 Å and that with I_n is 24.4Å (Fig. 1a). If we assume the height of the chlorite-like layer in the corrensite unit to be 14.14 Å (Drits et al., 2011), the residual thickness of smectite-like layer with I_w is 12.4 Å. Hence, I_w probably contains one atomic plane presumably consisting of water molecules and cations coordinated by the water molecules. Similarly, the height of the smectite-like layer with I_n interlayer is 10.2 Å. In the specimen, both two types of the smectite-like interlayers were observed with similar frequency, as shown in the several HRTEM images presented in this study. The two kinds of the corrensite units with the different smectite-like interlayers are finely interstratified (Fig. 1) or either is dominant in a view (I_w is dominant in Figure 2 whereas only I_n is observed in Figures 3 and 4). Transition between I_w and I_n, I_w and B-sheet, and I_n and B-sheet are also frequently recorded, as indicated by the white (I_n/I_w to B-sheet) and black (I_n to I_w) circles in Figure 1.

In previous works, the basal height of the corrensite unit observed in TEM was also varied between ca. 24 Å (Shau et al.,1990; Beaufort et al., 1997; Sugimori et al., 2008) and 26.5 Å (Murakami et al., 1999). It is a characteristic of the present specimen that the two heights coexist intimately. Drits et al. (2011) found that the XRD pattern of the present specimen in the air-dry state was well reproduced with three types of corrensite units whose heights are 29.00, 26.94 and 24.02 Å, with their proportion of 0.45 : 0.05 : 0.10, respectively though they all became 30.74 Å when treated with ethylene glycol. Hence, it is likely that the specimen contains smectite-like interlayers with different characters. Possible coexistence of 12.5Å and 10.2Å smectite-like layers in the present specimen is almost in agreement with the behavior of dioctahedral smectites in vacuum (Ferrage et al., 2005, 2007). In Ferrage et al. (2007), the layer thicknesses of the monohydrated (1W) and dehydrated (0W) smectite layers were 11.7 -12.0 Å and 10.0 Å, respectively. Because the layer thickness of 10.0 Å is larger than that of talc (9.35 Å) in which the interlayer is completely vacant, it was suggested that a certain amount of residual H_2O (or H_3O^+) was present in the interlayer related to 10.0 Å. In vacuum, generally the two kinds of smectite layers coexisted but the population of 1W layers was larger in the smectite specimen with higher layer charge (Ferrage et al., 2007). Hence, the two types of smectite(-like) interlayers observed in Ferrage et al. (2007) and the present specimen may reflect the difference of layer charge. Drits et al. (2011) reported that this specimen (sample 500L) is characterized by a high heterogeneity of cationic composition, from the electron microprobe analyses. This heterogeneity, which presumably causes variance of layer charge owing to the different amounts of tetrahedral aluminum, may correspond to the two types of smectite-like interlayers. However, as shown in Figure 1, the two types are interstratified with a monolayer level. It is not certain whether such fine interstratification really reflects the compositional difference.

Polytypic sequence in the corrensite units

Figures 2 and 3 show HRTEM images of corrensite along $\pm Y_i$ directions, where the basal height of the corrensite unit is mainly 26.5 Å (Fig. 2) and 24.4 Å (Fig. 3). First of all, it is evident that the contrasts of all 2:1 layers in the corrensite packets in these figures are identical, implying that mutual rotation with (±60°, 180°) does not occur with respect to the 2:1 layers (Kogure and Nespolo, 1999a, 1999b; Kogure et al., 2008). Next, HRTEM contrast at thin parts of the corrensite packets definitely shows the opposite directions of the octahedral slant between octahedral sheet in the 2:1 layer and B-sheet (Kogure and Banfield, 1998). Hence the polytypic stacking sequence of the chlorite-like

(DOI will not work until issue is live.) DOI: http://dx.doi.org/10.2138/am.2013.4314

layer in the corrensite unit should be II-types (II*aa*, II*bb* or II*ab*) among the six semi-random stacking sequences defined by Bailey and Brown (1962). These three sequences are distinguished in HRTEM images along the $\pm Y_i$-directions by the angle between the (001) plane and direction connecting the equivalent positions in the two 2:1 layers across the B-sheets (Kogure and Banfield, 1998). In Figures 2 and 3, these angles are all corresponding to that expected for II*bb* chlorite, indicating that the chlorite-like layer in the corrensite units adopts II*bb* stacking sequence.

On the other hand, an HRTEM image of corrensite along $\pm X_i$ direction is shown in Figure 4. In the figure, we denote the feature of stacking sequence in the chlorite layer (two 2:1 layers and B-sheet between them or TOT-B-TOT) in corrensite by the way used in Kameda et al. (2007), which originally presented in Baronnet and Kang (1989). First, we connect the closest dark spots at the two tetrahedral sheets in a 2:1 layer with a white bar (see, for instance, Kogure (2002) for the interpretation of the HRTEM contrast at the 2:1 layer). The slant of the bar with respect to the (001) plane corresponds to the projection of the intralayer displacement in the 2:1 layer (Guggenheim et al., 2009). If the slant direction is right-hand, the character "+" is given to the layer. If slanted to the left, it is designated with a "–", and if there is no slant, it is noted with a "0". Similarly, if the ends of the adjacent bars are shifted to right-hand, left-hand, or not shifted across the interlayer with B-sheet, which corresponds to the projection of the interlayer displacement (Guggenheim et al., 2009), the character "+","–", or "0" is given to the interlayer, respectively. Consequently, three characters, for instance " + – 0" around the bottom-left of the figure, are given to the chlorite layer (TOT-B-TOT) in the corrensite unit. In the figure, the projections of the intralayer displacements (or layer orientations) in the two 2:1 layers are always "+" and "0", whereas the interlayer displacement at the B-sheet is varied with "+" and "–".

These stacking features are expressed here using the symbolic notation by Zvyagin (Z-symbol) (1963, 1967). In Z-symbol, the character σ_n (n = 1 to 6) corresponds to the (001) projection of the vector connecting the center of the ditrigonal ring in the lower tetrahedral sheet to the octahedral M1 site in the upper octahedral sheet (or the M1 site to the center of the ditrigonal rings in the upper tetrahedral sheet), while the character τ_k (k =1 to 6) expresses the interlayer displacement between the adjacent tetrahedral sheets across the interlayer. In the idealized structure, the fractional *x* and *y* components for σ_1 and τ_4 are (a/3, b/3) ; for σ_2 and τ_5 are (–a/3, b/3) ; for σ_3 and τ_6 are (a/3, 0) ; for σ_4 and τ_1 are (–a/3, –b/3); for σ_5 and τ_2 are (a/3, –b/3), and for σ_6 and τ_3 are (–a/3, 0), respectively, where *a* and *b* are the parameters of the idealized based-centered unit cell. The three one-layer polytypes in chlorite belonging to II*bb* (II*bb*-2, II*bb*-4 and II*bb*-6) in Bailey and Brown (1962) can be expressed as $\sigma_6\tau_6\sigma_6$, $\sigma_2\tau_4\sigma_2$ and $\sigma_4\tau_2\sigma_4$, respectively, using Z-symbol (Zvyagin, 1967, Bailey, 1988b). However, in this study, the polytypic sequences are not restricted to the "one-layer" types and it is better to modify the expression for chlorite a little. In the original expressions, the origin of the stacking is at the octahedral M1 site. If the origin is changed to the center of the ditrigonal ring of the lower tetrahedral sheet, for instance, $\sigma_2\tau_4\sigma_2$ is expressed as $\sigma_2\sigma_2\tau_4$. Furthermore, $\sigma_2\sigma_2$ is equivalent to σ_5 if we assimilate the two σ symbols into one which corresponds to the intralayer displacement of a 2:1 layer. Consequently, II*bb*-2, II*bb*-4 and II*bb*-6 are expressed as $\sigma_3\tau_6$, $\sigma_5\tau_4$ and $\sigma_1\tau_2$, respectively.

As the HRTEM images along the $\pm Y_i$ directions (Figs. 2 and 3) show that the slant directions of all 2:1 layers are uniform, which means that the parity of n in σ_n is the same for all 2:1 layers. Here we can select odd parity for n without losing generality. On the other hand, the shifts between the two tetrahedral sheets across the B-sheet are also uniform and the same direction as the slants of the 2:1 layers. Hence, the parity of k in τ_k is the same for all chlorite-like interlayers and different from n in σ_n, namely even parity. Next, the stacking sequences appeared in the HRTEM image along the $\pm X_i$ direction (Fig. 4) will be expressed with Z-symbol. If we assume that the beam direction is antiparallel to the **a**-axis, the sequence "+ – 0" corresponds to $\sigma_5\tau_4\sigma_3$. Similarly "+ + 0" corresponds to $\sigma_5\tau_2\sigma_3$. It is understood that the stacking sequence $\sigma_5\tau_4\sigma_3$ is the combination of II*bb*-4 ($\sigma_5\tau_4$) and II*bb*-6 ($\tau_2\sigma_1$), because if the vectors $\tau_2\sigma_1$ are rotated counterclockwise by 120°, they are expressed as $\tau_4\sigma_3$. Similarly, $\sigma_5\tau_2\sigma_3$ is regarded as the combination of II*bb*-2 and II*bb*-4. As summary, the stacking sequence of TOT-B-TOT unit in the corrensite packets is expressed by the combination of different polytypes in II*bb*.

One may insist to analyze the stacking sequence of whole layers in the corrensite unit, including the smectite-like interlayer from Figures 2 to 4. However, it seems not important due to two reasons. First, the structure of the smectite-like interlayer is "artificial" in a sense, formed by collapse in the vacuum environment and may have little to do with the original structure when the corrensite was formed. Secondly, it is still not certain, for instance, whether the interlayer displacement at the collapsed smectite-like interlayer has certain directions or lengths like chlorite-like interlayer with B-sheet. It is evident that HRTEM contrast is not so accurate to unambiguously determine these directions and lengths.

Transition from corrensite to chlorite

Beside the frequent observation of transition between the smectite-like interlayer and B-sheets as shown in Figure 1, additional evidences support the assumption that the chlorite packets were transformed from corrensite in this specimen *via* the conversion of the interlayer structure. For instance, the numbers of successive B-sheets in the chlorite packets are always odd-numbered (Fig. 5), as predicted in Drits et al. (2011). This is definitely accountable by the transition from corrensite to chlorite by replacing smectite-like interlayers with B sheets (Fig. 6). This transition mechanism also limits the minimum packet of chlorite to three layers, which will contribute the result of the XRD simulation in which chlorite and corrensite tend to segregate (P_{chch} = 0.75 for 40% chlorite) in the present specimen (Drits et al., 2011).

If the conversion of the interlayer is the pathway from corrensite to chlorite, the stacking sequence in corrensite should be inherited. For instance, HRTEM images of the chlorite packets along the $\pm Y_i$ directions indicate that the packet clearly has the II*bb* polytypic character (Fig. 7), which must inherit the same stacking sequence of the chlorite layer in corrensite (Figs. 2 and 3). Moreover, the "two-layer" character with respect to the orientation of the 2:1 layer in corrensite (Fig. 4) was also found in chlorite packets (Fig. 8). In the figure, only three 2:1 layers violate the "two-layer" character of the layer orientation (alternating σ_5 and σ_3) among twenty-seven layers in the image. On the other hand, the interlayer displacements (τ_k) are almost random. According to the transformation process suggested here, the alternating chlorite interlayers were converted from the smectite-like interlayers in corrensite. Although the new chlorite-like interlayers adopted II*bb* because this sequence is considered energetically most stable, further regulation (preference among τ_2, τ_4 or τ_6) did not occur because of their similar formation energies. Moreover, τ_k for the chlorite-like interlayer in the original corrensite is also not ordered, as shown in Figure 4. In spite of the disorder of τ_k and partial disorder of σ_n, the stacking of chlorite in Figure 8 is very unique and it definitely comes from that this chlorite was converted from corrensite via the transition pathway as described above. It is interesting that Shau and Peacor (1992) reported a HRTEM image of chlorite to show a "two-layer" periodicity, in a specimen (hydrothermally altered basalt) where corrensite and chlorite coexist. Analyses of the stacking sequence using HRTEM as demonstrated in the present study will bring us further understanding for the smectite-corrensite-chlorite transition in variable geological environments.

CONCLUDING REMARKS

As mentioned above, this work started to verify the results of our XRD analyses for the present sample (Drits et al., 2011). The high content of chlorite layers and the particular character of their distribution among corrensite layers observed in the HRTEM images are in a perfect agreement with those determined by modeling of the XRD pattern. It turned out therefore that 40% chlorite layers distributed with a certain tendency to segregation with 60% ethylene-glycolated corrensite layers produce the XRD pattern with the almost rational set of basal reflections. It means that Bailey' criterion (Bailey, 1992) cannot be used alone for identification of corrensite. In addition, the studied corrensite structure consists of different types of smectite-like interlayers, identified both by HRTEM in vacuum (the present study) and by XRD in air-dried state (Drits et al., 2011). Finally, it was demonstrated that the model should include a set of intermediate mixed-layer members in which several layer types are interstratified not only from a pure random to completely ordered structures as was accepted previously, but also from random to completely segregated structures as was found by XRD and HRTEM in the present work. It is worth insisting that only such a rigorous model including the actual number, content, and distribution of the various layer types can reproduce with a high quality positions, intensities, and profiles of basal reflections in the experimental XRD pattern of the mixed-layer minerals .

The present work has also reported for the first time the three dimensional stacking structure of corrensite, including II*bb* type stacking sequence of the chlorite-like layers and a "two-layer" polytypic character for the two 2:1 layers in the corrensite unit. These regulated features of corrensite structure can be a strong evidence that corrensite has a particular thermodynamic stability field, as proposed in previous works. Moreover, such a "two-layer" character indicates that corrensite in this study precipitated directly from solution (probably in an environment with a high water/rock ratio), without inheriting the smectite structure in which such regular stacking is generally not expected. On the other hand, the odd number of the successive B-sheets in the mixed-layer Co-C structure along with the similarity of the polytypic stacking sequences between corrensite and chlorite can be considered as the evidence of the transition from corrensite to chlorite by replacing the smectite-like interlayers with B-sheets. Of course, the structural features described here may not be extended to other corrensite and corrensite–containing specimens formed in different geological environments, and it is our future works to investigate them based on methodologies applied to the present sample. Investigation with accurate XRD and HRTEM analyses will give better understanding for the formation mechanism of corrensite and its conversion path ways in various physico-chemical conditions.

Acknowledgments

First of all, we are grateful to T. A. Ivanovskaya to prepare sufficient amount of the monomineral corrensite-chlorite specimen. We also thank to E. Fujii for the preparation of the TEM specimens. The quality of the paper has been significantly improved by the valuable comments by R.F. Yuretich and A. Baronnet. This work was supported by Grants-in-Aid for Scientific Research 24340133 and 21107005 from the Japan Society for the Promotion of Science (JSPS) and Ministry of Education, Culture, Sports, Science and Technology (MEXT), respectively. A part of this work was supported by the Russian Foundation for Basic Research (project Nos. 12-05-00234).

References

Bailey, S.W. and Brown, B.E. (1962) Chlorite polytypism: I. Regular and semi-random one-layer structures. American Mineralogist, 47, 819–850.

Bailey, S.W. (1982) Nomenclature for regular interstratifications, American Mineralogist, 67, 394-398.

Bailey, S.W. (1988a) X-ray diffraction identification of the polytypes of mica, serpentine, and chlorite. Clays and Clay Minerals, 36, 193–213.

Bailey, S.W. (1988b) Chlorites: structure and crystal chemistry. Ch. 10 in: Hydrous phyllosilicates, Bailey, S.W. (Ed.) Vol. 19, Reviews in Mineralogy, Mineralogical Society of America, 225-280.

Banfield, J.F. and Bailey, S.W. (1996) Formation of regularly interstratified serpentine-chlorite minerals by tetrahedral inversion in long-period serpentine polytypes. American Mineralogist, 81, 79-91.

Banfield, S.W. and Murakami, T. (1998) Atomic-resolution transmission electron microscope evidence for the mechanism by which chlorite weathers to 1 : 1 semi-regular chlorite-vermiculite, American Mineralogist, 83, 348-357.

Baronnet, A. and Kang, Z.C. (1989) About the origin of mica polytypes. Phase Transitions, 16/17, 477-493.

Beaufort, D., Baronnet, A., Lanson, B. and Meunier, A. (1997) Corrensite: A single phase or a mixed-layer phyllosilicate in the saponite-to-chlorite conversion series? A case study of Sancerre-Coy deep drill hole (France), American Mineralogist, 82, 109-124.

Bettison, L.A. and Schiffman, P. (1988) Compositional and structural variations of phyllosilicates from the Point Sal ophiolite, California, American Mineralogist 73, 62-76.

Bettison-Varga, L. and Mackinnon, I.D. (1997) The role of the randomly mixed-layered chlorite/smectite in the transformation of smectite to chlorite. Clays and Clay Minerals, 45, 506-516.

Bons, A.J. and Schryvers, D. (1989) High-resolution electron microscopy of stacking irregularities in chlorites from the central Pyrennes. American Mineralogist, 74, 1113-1123.

Chang, H.K., MacKenzie, F.T. and Schoonmaker, J. (1986) Comparison between the diagenesis of dioctahedral and trioctahedral smectite, Brazilian offshore basins. Clays and Clay Minerals, 34, 407-423.

Drits, V.A. and Kossovskaya, A.G. (1990) Clay minerals: smectites and mixed-layer minerals. Moscow: Nauka, 212pp (in Russian)

Drits, V.A. and Sakharov, B.A. (1976) The X-Ray diffraction analysis of mixed-layer minerals. Moscow: Nauka, 255pp (in Russian)

Drits, V.A., Ivanovskaya, T.A., Sakharov, B.A., Zviagina, B.B., Gor'kova, N.V., Pokrovskaya, E.V. and Savichev, A.T. (2011) Mixed-layer corrensite-chlorite and their formation mechanism in the glauconitic sandstone-clayey rocks (Riphean, Anabar Uplift), Lithology and Mineral Resources, 46, 566-593.

Ferrage, E., Lanson, B., Sakharov, B.A., Geoffroy, N., Jacquot, E., and Drits, V.A. (2005) Investigation of dioctahedral smectite hydration properties by modeling of X-ray diffraction profiles: Influence of layer charge and charge location. American Mineralogist, 92, 1731-1743.

Ferrage, E., Lanson, B., Sakharov, B.A., and Drits, V.A. (2007) Investigation of dioctahedral smectite hydration properties by modeling experimental X-ray diffraction patterns: Part I. Montmorillonite hydration properties. American Mineralogist, 90, 1358-1374.

Guggenheim, S., Adams, J. M., Bergaya, F., Brigatti, M., Drits, V. A., Formoso, M., Galan, E., Kogure, T., Stanjek, H. and Stucki, J.W. (2009) Nomenclature for stacking in phyllosilicates: report of the association international pour l'etude des argiles (AIPEA) nomenclature committee for 2008. Clays and Clay Minerals, 57, 134–135.

Inoue, A. (1987) Conversion of smectite to chlorite by hydrothermal diagenetic alterations, Hokuroku Kuroko Mineralization area, Northeast Japan, *Proc. Of the International Clay Conference, Denver. Clay Mineral Society*, vol. 8, 158-164.

Inoue, A. and Utada, M. (1991) Smectite-to-chlorite transformation in thermally metamorphosed volcanoclastic rocks in the Kamicita area, Northem Honshu, Japan. American Mineralogist, 76, 628-640.

Inoue, A., Utada, M., Nagata, H. and Watanabe, T. (1984) Conversion of trioctahedral smectite to interstratified chlorite/smectite in Pliocene acidic pyroclastic sediments of the Ohyu district, Akita Prefecture, Japan. Clay Science, 6, 103-116.

Kameda, J., Miyawaki, R., Kitagawa, R. and Kogure, T. (2007) XRD and HRTEM analyses of stacking structures in sudoite, di-trioctahedral chlorite. American Mineralogist, 92, 1586-1592.

Kilaas, R. (1998) Optical and near-optical filters in high-resolution electron microscopy. Journal of Microscopy, 190, 45-51.

Kogure, T. (2002) Investigation of micas using advanced TEM. in “Micas: Crystal Chemistry & Metamorphic Petrology, Reviews in Mineralogy and Geochemistry Vol. 46”, A. Mottana, F.P. Sassi, J.B. Thompson, JR., S. Guggenheim, ed. Mineralogical Society of America, Washington, D.C., 281-312.

Kogure, T. and Banfield, J.F. (1998) Direct identification of the six polytypes of chlorite characterized by semi-random stacking. American Mineralogist, 83, 925-930.

Kogure, T. and Banfield, J.F. (2000) New insights into the mechanism for chloritization of biotite using polytype analysis. American Mineralogist, 85, 1202-1208.

Kogure T, and Murakami T (1996) Direct identification of biotite/vermiculite layers in hydrobiotite using high-resolution TEM. Mineral Journal, 18, 131-137

Kogure, T. and Murakami, T. (1998) Structure and formation mechanism of low-angle grain boundaries in chlorite. American Mineralogist, 83, 358–364.

Kogure, T. and Nespolo, M. (1999a) A TEM study of long-period mica polytypes: determination of the stacking sequence of oxybiotite by means of atomic resolution images and Periodic Intensity Distribution (PID). Acta crystallographica. Section B, Structural science, 55, 507-516.

Kogure, T and Nespolo, M (1999b) First occurrence of a stacking sequence including (+/- 60 degrees,180 degrees) rotations in Mg-rich annite. Clays and Clay minerals, 47, 784-792.

Kogure, T., Eilers, P.H.C., and Ishizuka, K. (2008) Application of optimum HRTEM noise filters in mineralogy and related sciences. Microscopy and Analysis, 22, S11-S14.

Kossovskaya, A.G. and Drits, V.A. (1975) Crystal chemistry of dioctahedral micas, chlorites, and corrensites as indicators of geological setting. In: Crystal chemistry of minerals and geological problems. Ed. Kossovskaya, A.G. Moscow: Nauka, 60-69 (in Russian)

Leoni, L., Lezzerihi, M., Battaglia, S. and Cavalcante, F. (2010) Corrensite and chlorite-rich Chl-S mixed layers in sandstones from the 'Macigno' Formation (northwestern Tuscany, Italy), Clay Minerals, 45, 87-106.

Marks, L.D. (1996) Wiener-filter enhancement of noisy HREM images. Ultramicroscopy, 62, 43-52.

Murakami, T., Sato, T. and Inoue, A. (1999) HRTEM evidence for the process and mechanism of saponite-to-chlorite conversion through corrensite, American Mineralogist, 84, 1080-1087.

Reynolds, R.C. Jr. (1980) Interstratified clay minerals. Ch. 3. In: Crystal Structures of Clay Minerals and their X-ray identification, G.W. Brindley and G. Brown eds. Mineralogical Society, London.

Reynolds, R.C. Jr. (1985) NEWMOD© a computer program for the calculation of one-dimensional diffraction patterns of mixed-layered clays. R.C. Reynolds, 8 Book Rd., Hanover, New Hampshire 03755, U.S.A.

Reynolds, R.C. Jr. (1988) Mixed layer chlorite minerals. Ch. 15 in: Hydrous phyllosilicates, Bailey, S.W. (Ed.) Vol. 19, Reviews in Mineralogy, Mineralogical Society of America, 601-629.

Shau, Y-H. and Peacor, D.R. (1992) Phyllosilicates in hydrothermally altered basalts from DSDP Hole 504B, Leg 8 3- a TEM and AEM study. Contributions to Mineralogy and Petrology, 112, 119-133.

Shau, Y-H., Peacor, D.R. and Essene, E.J. (1990) Corrensite and mixed-layer chlorite/corrensite in metabasalt from nortahn Taiwan: TEM/AEM, EPMA, XRD, and optical studies, Contribution to Mineralogy and Petrology, 105, 123-142.

Sugimori, H., Iwatsuki, T. and Murakami, T. (2008) Chlorite and biotite weathering, Fe^{2+}-rich corrensite formation, and Fe behavior under low P_{O2} conditions and their implication for Precambrian weathering, American Mineralogist, 93, 1080-1089.

Velde, B. (1977) A proposed phase diagram for illite, expanding chlorite, corrensite and illite-montmorillonite mixed layered minerals. Clays and Clay Minerals, 25, 264-270.

Zvyagin, B. B. (1963) The theory of chlorite polymorphism. Kristallografya, 8. 12-38.

Zvyagin, B. B. (1967) Electron-diffraction analysis of clay mineral structures. Prenum Press, New York, 364p.

Figure captions

Figure 1. (a) HRTEM image of corrensite-chlorite interstratification. The arrowheads with "B", "I_w", and "I_n" indicate the positions of the interlayers with the brucite-like sheet, smectite-like interlayer with one atomic plane, and that with no distinct material, respectively. The white circles show the areas with transition between the brucite-like sheet and smectite-like interlayer, whereas the black circles indicate the transition between I_w and I_n at the smectite-like interlayer. (b) Magnified image around the center of (a) to show two types of the smectite-like interlayer with I_w and I_n. (c, d) Magnified images at the squares around arrows "1" (c) and "2" (d). The 2:1 layers above the arrow "1" show a 4.5 Å periodicity along the layers (c), indicating the beam direction close to $\pm X_i$ direction. On the other hand, the several layers below the arrow "2" show a 2.6 Å periodicity (d), indicating the direction close to $\pm Y_i$.

Figure 2. (a) Filtered HRTEM image of corrensite recorded along the $\pm Y_i$ direction. The smectite-like interlayers in the image are all I_w type except one indicated with "I_n". (b) Magnified image at the white square in (a). The arrowheads with "T" and "O" indicate the tetrahedral and octahedral sheets in a 2:1 layer, respectively (see Kogure and Banfield, 1998). The other symbols are the same as those in Figure 1. The white thin lines indicate the expected angles between the (001) plane and the line connecting the equivalent positions in the adjacent 2:1 layers across the B-sheets for II*bb* chlorite. The inset is the simulated image for II*bb* chlorite along the [010] direction. See Kogure and Banfield (1998) for the parameters used in the simulation.

Figure 3. (a) Filtered HRTEM image of a corrensite packet recorded along the $\pm Y_i$ direction. The smectite-like interlayers in the image are all I_n type. The contrast at the thin region indicates that the slant directions of the octahedra in the 2:1 layer and that in the B-sheet are opposite. The white thin lines indicate the angle between the (001) plane and the line connecting the equivalent positions in the adjacent 2:1 layers across B-sheets, expected for II*bb* chlorite. Note that the white lines between adjacent layers connect equivalent dark spots in the tetrahedral sheets, concluding that the stacking sequence across the brucite-like sheet is II*bb*.

Figure 4. Filtered HRTEM image of corrensite recorded along the $\pm X_i$ direction. The crystal was considerably damaged by electron radiation during observation and recording. The smectite-like interlayers in the image are all I_n type with the 24 Å height for the corrensite unit. The white bar for each 2:1 layer connects the closest dark spots in the two tetrahedral sheets in a 2:1 layer and characters "+", "–" and "0" correspond to the slant of the bar and lateral shift of the bars across the interlayer (see the text).

Figure 5. One-dimensional HRTEM images of corrensite-chlorite interstratifications. The black arrows indicate the positions of B-sheets. Notice that numbers of successive B-sheets in the chlorite packets (indicated with the square blackest) are all odd, as indicated on the brackets.

Figure 6. Schematic drawing to show the formation of the chlorite packet in corrensite by replacing the smectite-like interlayers with B-sheets, as indicated by the arrows. Note that the number of successive B-sheets in the growing chlorite packet in the bracket is always odd.

Figure 7. Filtered HRTEM image of a chlorite packet along the $\pm Y_i$ directions. The Fourier transform of the image is shown at the top-left and the magnified image at the white square at the top-right. The opposite slant directions between the octahedral sheet in the 2:1 layer and B-sheet, and the feature in the Fourier transform indicate that the stacking in the chlorite is II*bb* (Kogure and Banfiled, 1998).

Figure 8. Filtered HRTEM image of a thick chlorite packet, viewed along the $\pm X_i$ direction. The white bar at each 2:1 layer connects the closest dark spots in the two tetrahedral sheets in a layer, to show the orientation of the 2:1 layer. The characters "0", "+" or "–" in the left rows correspond to the direction of the slant of the white bar ("0" corresponds to no slant, "+" to slant to the left, "–" to right) for each 2:1 layer, while those in the right row indicate the shift between the bars across the interlayer (see the text).

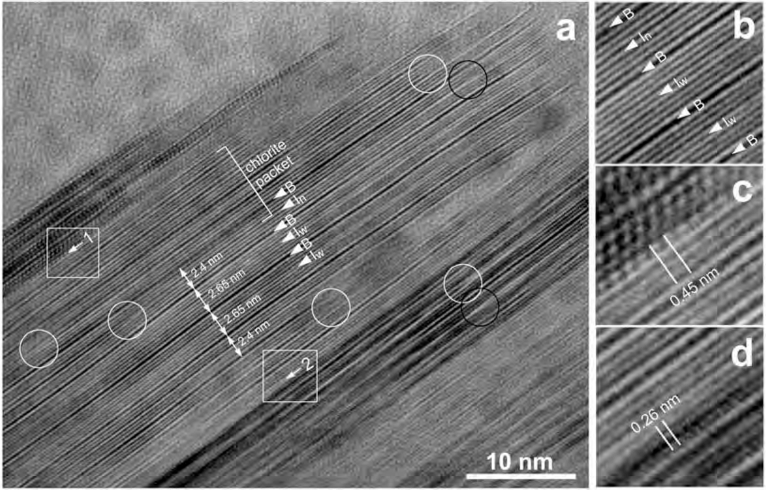

Kogure et al., Figure 1

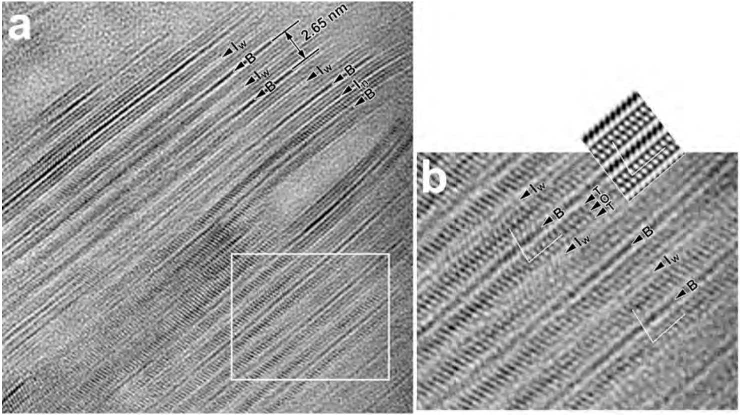

Kogure et al., Figure 2

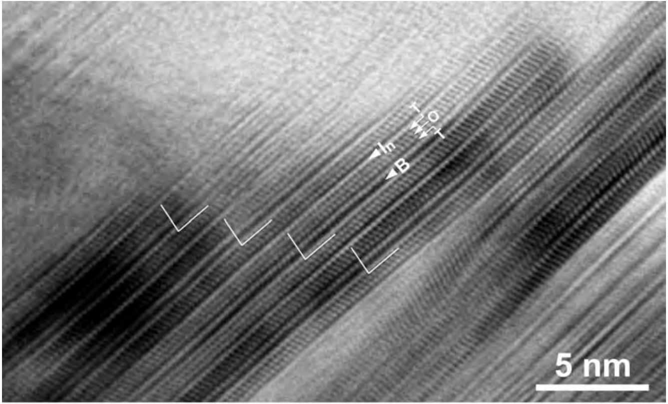

Kogure et al., Figure 3

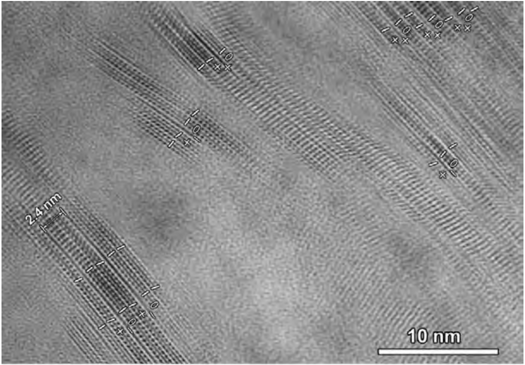

Kogure et al., Figure 4

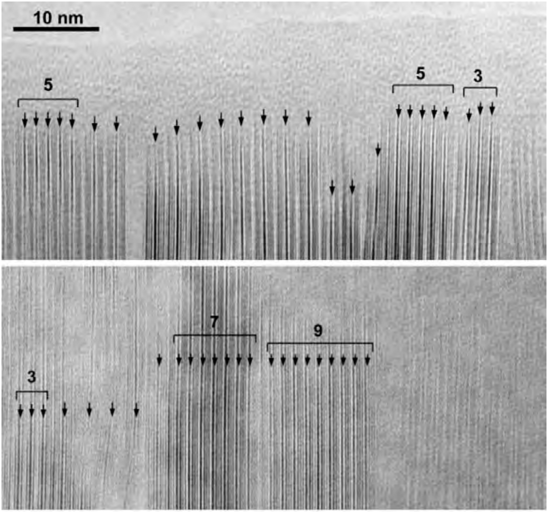

Kogure et al., Figure 5

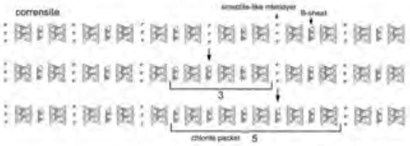

Kogure et al., Figure 6

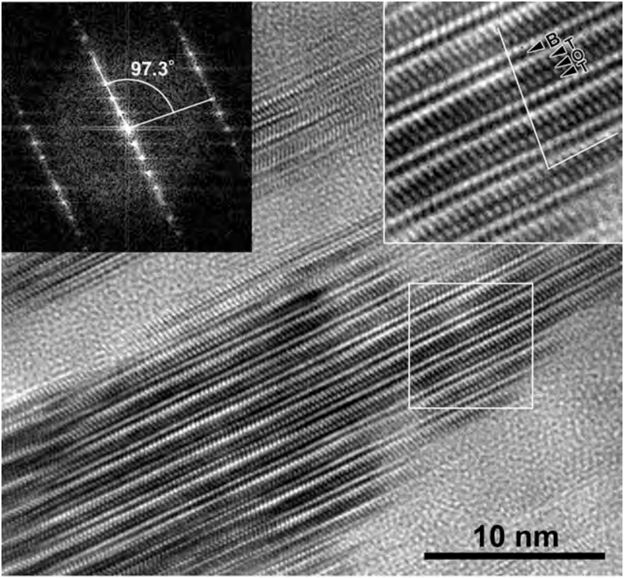

Kogure et al., Figure 7

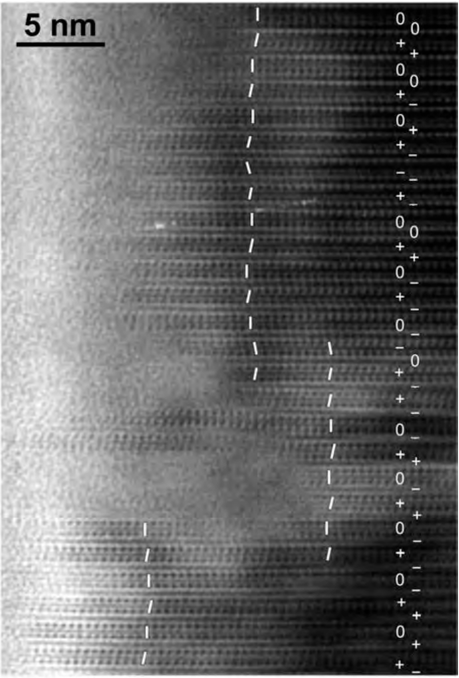

Kogure et al., Figure 8